

A CONTROL PARADIGM FOR DECOUPLED OPERATION OF MOBILE ROBOTS IN REMOTE ENVIRONMENTS

Remo Pillat¹, Charles E. Hughes¹, and Arjun Nagendran¹

*Institute for Simulation and Training, University of Central Florida, 3100 Technology Pkwy, Orlando, FL, U.S.A.
{rpillat, ceh, arjun}@cs.ucf.edu*

Keywords: Mobile Robots, Tele-operation, Virtual Environments, Robot Simulation

Abstract: Remote operation of robots in distant environments presents a significant challenge for direct control due to inherent issues with latency and available bandwidth. Purely autonomous behaviors in such environments come with the associated risks of failure. It may be advantageous to acquire information about the environment from the robot's onboard sensors, to re-create a simulation and plan a mission beforehand. The planned mission can then be uploaded to the robot for execution, allowing the physical robot to handle the autonomy required for completing its task. In this paper, the foundations of a control paradigm are presented that uses a simulated virtual environment to decouple the operator from the physical robot, thus circumventing latency problems. To achieve this, it is first required to accurately model the robot's kinematic parameters for use in the simulation. Kalman filtering techniques that demonstrate this modeling for a differential drive robot are presented in this paper. The estimated parameters are then used as inputs to a modular planning and execution module. Based on simulation results, a safe and non-redundant path can then be uploaded and executed on the real robot.

1 INTRODUCTION

Robots have become a ubiquitous presence in today's society. They have found uses in diverse areas such as manufacturing, health care, planetary exploration, and entertainment. Autonomous operation of these robots is usually limited to processes that occur in controlled environments and involve repetitive steps, e.g. the assembly of cars.

Whenever a robot is deployed on a remote mission, some form of tele-operation has to be employed. Conventionally, tele-operation refers to the direct control of a robot from a remote location using onboard sensors that provide the required navigational aids. In mobile robotics this need is most pronounced in exploring areas that are hazardous or inaccessible to humans, e.g. when surveying a stricken nuclear plant or controlling a rover on a different planet. Recently, the medical community has made long strides towards making minimally invasive robotic surgery a routine procedure, but in most commercially available systems the operator has to be located in close physical proximity. Remote tele-operation is however always hampered by the inescapable bandwidth limitations and communication time delays (latency).

Transmission delays and bandwidth limitation are

an unavoidable feature of long-distance communication. These must be compensated for within existing control schemes or an alternative control paradigm must be applied. In this work, an architecture will be presented that decouples the operator's actions (master) on a simulated robot from the executed actions on the real robot (slave) through a virtual reality-based simulation layer. The general control paradigm is based on the following assumptions that are not presented in the scope of this paper.

- The simulation environment can be constructed by gathering real-world data through the robot's onboard sensors and is sufficiently representative within a localized region around the robot
- The real robot has sufficient autonomy to be able to execute a mission plan under the influence of external uncertainties, or report discrepancies that prevent execution

An operator can work in the simulation environment to plan and execute his mission either by controlling the robot manually, or experiment with higher level autonomous planning modules. Once mission execution in simulation is completed, a set of modules process the simulation data to re-create a mission plan for the real robot. The modules are capable of accepting user inputs to prioritize the mission's goals and

remove any redundancy in the simulated mission. A newly created mission plan is then uploaded to the real robot for execution. The work presented herein focuses on the use of Kalman filtering techniques to determine the robot's kinematic parameters and the role of the different modules in the decoupling process.

2 BACKGROUND

Traditionally, bilateral tele-operation with time delays requires specialized control schemes to assure system stability and transparency. Good surveys of these methods can be found in (Arcara and Melchiorri, 2002) and (Hokayem and Spong, 2006).

All of these methods try to address the problem of direct control of the slave by the master under the presence of time delay. If the time delays are highly variable or impractical to the operators other methods have to be employed. (Pan et al., 2006) takes a new approach by proposing a dual predictor/observer control scheme on both the master as well as the slave side, thus circumventing the usage of any delayed information.

In one of the earliest attempts for an alternative paradigm, (Bejczy et al., 1990) displays a virtual "phantom robot" on the master side that can be controlled directly without time delay. In these experiments the real robot arm follows the phantom movements with the implicit time delay. Unfortunately, this scheme increases the execution time of any motion, because the operator will perform a motion on the phantom robot and then has to wait until the real robot attains the same configuration. (Kheddar, 2001) first introduced the "hidden robot concept" that completely abstracted the movements of the real robot from the operator by only presenting him with a virtual presentation.

(Kheddar et al., 2007) provides a more recent survey of the state-of-the-art in using virtual reality simulations to overcome the inherent tele-operation limitations. Closely related to our work is the emerging field of Teleprogramming (Hernando and Gambao, 2007) where the operator does not directly control the robot, but a simulated copy. After an action is executed, an abstract command sequence that signals operator intent is sent to the slave robot. The authors make an effort to abstract the underlying system variables on the master and slave side and only transmit operator intentions. This approach is laudable in its generalizing power, but has implicit requirements of accurate simulation models for robots and the environment.

With exception of (Wright et al., 2006) and (Yu et al., 2009), many teleprogramming systems focus on the operation of robot arms, while systems tailored towards mobile robot tele-operation have gained less attention. This might be due to the fact that the physical simulation of mobile robots dynamics and environment interaction is non-trivial.

Professional robot simulators have sufficiently advanced to provide a satisfactory simulation of physical interactions between robot and the environment. Examples of commercial systems include Marilou (Anycode, 2011), Webots (Michel, 2004), and Microsoft Robotics Studio (Jackson, 2007).

Predictive simulators have also been used to allow multi-robot coordinating missions as in (Chong et al., 2000).

3 SYSTEM ARCHITECTURE

As stated previously, transmission delays, missing communication packets, and bandwidth limitation are an unavoidable feature of long-distance communication. Communication latencies beyond several hundred milliseconds are generally unacceptable for human operators and produce dangerous control instabilities. This paper proposes an architecture that decouples the operator's actions from the executed motions of the robot. This has several advantages that can not be achieved in traditional tele-operation. Given a representation of the environment, operators can plan and execute simulated missions without the need for a permanent communication connection to the physical robot. Time-intensive trial runs can be shortened, while invalid inputs and redundancies can be corrected before any commands are uploaded to the real robot.

The general control infrastructure will support both goals of visual and operational fidelity on the master's side as well as tight closed-loop control without time delay by the slave (Figure 1).

At the highest level, our Master-Slave Control Architecture (Zhu et al., 2011) features a simulation server that maintains an environmental model and simulated robotic entities with sensors and actuators. All simulation components are based on the commercial Marilou robotics simulator (Anycode, 2011). Without a physical complement, a program can be launched locally that controls the movements of the robot in the simulated environment. This is the master layer and it can function independently of any other communication.

The uniqueness of the control architecture lies in decoupling the networked layers. The simulation

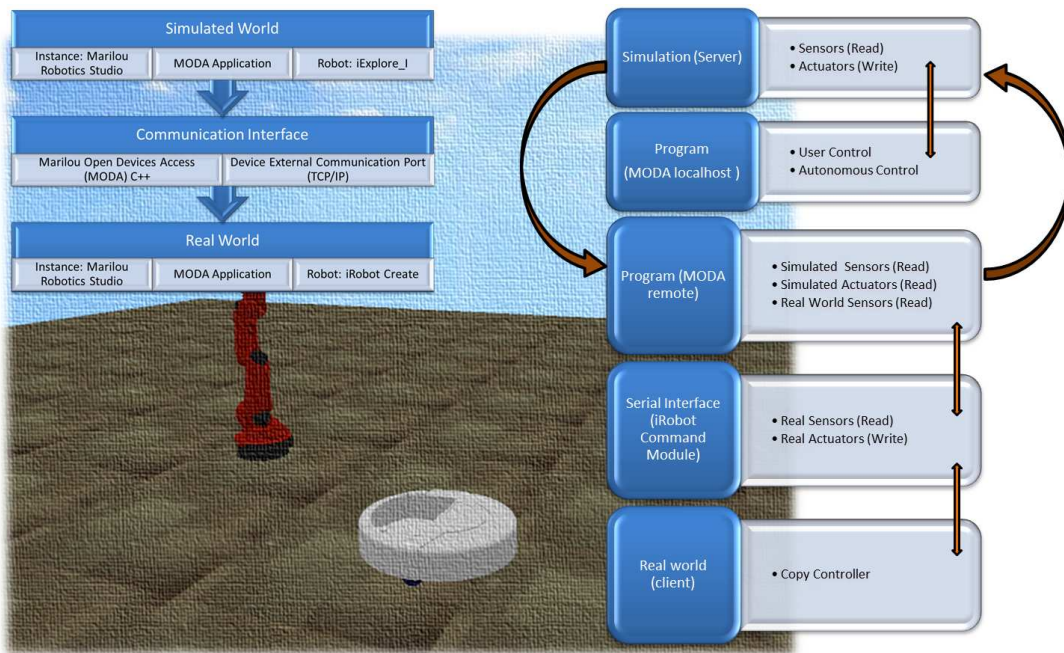


Figure 1: General architecture of the control paradigm

layer is used to plan and execute movements beforehand. These planned movements guide the real robot that attempts to closely follow the simulated robot without the need for explicit user control, while maintaining a degree of autonomy to cope with dynamically changing situations.

A remote program residing on the slave in the real world connects to the Master and reads the values from the simulated sensors / actuators. The communication interface then translates the actuator commands to the real-robot (slave). At the same time, real world sensors are read and data is fed back to the simulation establishing a bilateral communication interface; discrepancy in the received data from that predicted by the simulation causes control to be transferred back to the Master.

The strength of the presented system, in comparison to the predictive simulation systems mentioned in section 2, is its inherent ability to initially identify and continually update the simulated representation of the robot. Previous work relied heavily on a priori available simulation models or overly simplified physical modeling. In addition, the modularity of the architecture allows easy addition of high-level planning or processing modules.

While interpreting sensor data to recreate a simulation dynamically forms one component, it is equally important to have a robust model of the robot itself in the simulation. Section 4 will focus on the use of Kalman filtering techniques to estimate the robot's

kinematic parameters for use in simulation. These estimates are then passed as inputs to the modular planning and execution system which processes the simulated data to generate a feasible mission plan for the real robot (see Section 5). The significance of estimation errors in these parameters on the simulation are highlighted in Section 6.

4 KINEMATIC ROBOT SIMULATION MODEL

An accurate kinematic model of the controlled entity is essential for any predictive simulation of robot motions. The existence and accuracy of this model is an a priori requirement for both the validity of the physical simulation in the master virtual environment as well as the legitimacy of any simulated planning action.

In existing systems that demonstrated the teleoperation of mobile robots, for example (Yu et al., 2009) and (Wright et al., 2006), this robot model is assumed to be provided to the simulator with sufficient accuracy. In most cases, the parameters of this model are hard to quantify, because values from manufacturer's specifications or manual measurements are either non-existent, prone to errors, or can vary from one robot to the next. Through the example in Section 6 it will be convincingly argued that even small

changes of the robot's kinematic variables have a strong influence on the accuracy of the motion simulation in the planning and execution stages. For any system employing a simulated mobile robot, this fact cannot be overstated, because in the overall system architecture many higher level modules will depend on the precision of the kinematic parameters.

This makes the need for an automatic calibration method more pronounced. In this section, the kinematic model of the well-known differential drive configuration will be developed. In addition, a unified framework for the automatic identification of the kinematic parameters of a differential-drive robot will be presented that allows off-line as well as online estimation. Ideally, this process will be self-calibrating and should not require any human control input beyond a rough initial value of the estimated entities.

4.1 Basic Differential Drive Model

The differential drive configuration is a commonly encountered mobile robot combination that uses two actuated wheels and one or more (passive) casters. For the purposes of this work the parameters of this configuration can be simplified according to Figure 2.

The kinematic parameters that should be estimated are the diameters of the left and right wheels (d_L and d_R , respectively), and the wheel base b .

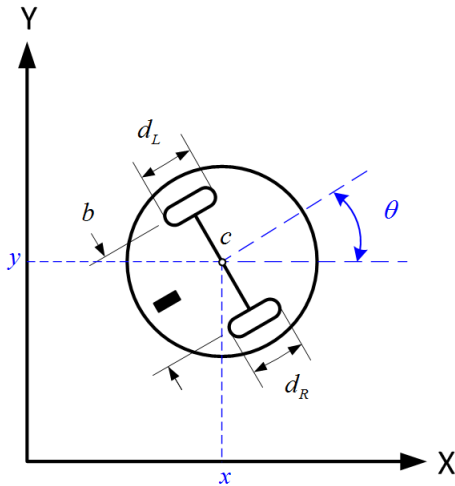


Figure 2: Differential drive configuration. Here d_L and d_R denote the diameters of the left and right wheel, respectively. c is the center point between the actuated wheels and b is the wheelbase.

When the robot moves in 2D its basic state at time instant k can be described by $\mathbf{x} = [x, y, \theta]^T$. Here the coordinates (x, y) denote its position and θ the orientation of its body.

Depending on the sampling time, the movement of a differential drive robot can be approximated either by a linear motion or, more generally, a circular arc. Following the derivation for the latter case outlined in (Wang, 1988), the state transition between time steps k and $k + 1$ can be described as follows:

$$\mathbf{x} = \begin{bmatrix} x_{k-1} \\ y_{k-1} \\ \theta_{k-1} \end{bmatrix} + \begin{bmatrix} \frac{\sin(\alpha)}{\alpha} \Delta s \cos(\theta_{k-1} + \alpha) \\ \frac{\sin(\alpha)}{\alpha} \Delta s \sin(\theta_{k-1} + \alpha) \\ \Delta \theta_k \end{bmatrix} \quad (1)$$

Here Δs denotes the distance that the center c of the robot traverses along the circular arc. The change in orientation is signified by $\Delta \theta_k$. $\alpha = \Delta \theta_k / 2$ is simply the half angle of the orientation change.

4.2 Incorporating Odometry Readings

In most cases, the odometry of the robot is derived from encoders that are mounted on the driveshaft of the actuated wheels. Even if they are not equipped on a mobile base, they can easily be retrofitted.

Let e_{res} be the encoder resolution per wheel rotation. This value is constant and assumed to be known. The encoder count differences between time steps are indicated by Δe_L for the left wheel and Δe_R for the right one.

Then the values for Δs and $\Delta \theta$ in Equation (1) can be reformulated (under no wheel-slip conditions) as:

$$\Delta s = \frac{\Delta s_R + \Delta s_L}{2} = \frac{\pi(d_L \Delta e_L + d_R \Delta e_R)}{2 e_{res}} \quad (2)$$

$$\Delta \theta = \frac{\Delta s_L - \Delta s_R}{b} = \frac{\pi(d_L \Delta e_L - d_R \Delta e_R)}{e_{res} b} \quad (3)$$

Δs_L is the distance traveled by the left wheel and Δs_R the equivalent quantity for the right wheel.

These derived equations will be used for estimating the state of the robot between time steps. Because the robot state depends on our kinematic unknowns, they can be estimated continuously while the robot drives an arbitrary path.

4.3 Online Estimation

For estimating the state of a linear system, the Kalman Filter (Kalman, 1960) and its many derivatives have been the de facto standard in the robotics community. Under the assumption that all state variables are perturbed by zero-mean normal-distributed noise, the Kalman Filter is an optimal recursive estimator for the state variables of linear dynamical systems.

As can readily be seen by inspecting Equation (1), the state transition between samples is described by

nonlinear equations. To handle that, this paper will use the Extended Kalman Filter (Julier and Uhlmann, 2004), which linearizes the state transition equations around the current mean and covariances of the estimated quantities.

Akin to the state description in Section 4.1, our state vector is \mathbf{x} , but the process is now governed by the non-linear function f :

$$\mathbf{x}_k = f(\mathbf{x}_{k-1}, \mathbf{w}_k) \quad (4)$$

Here, the non-linear function f relates the state \mathbf{x}_{k-1} from the last time step and process noise $\mathbf{w}_k \sim N(0, Q)$ to the current state.

A vector of measurements can be calculated by:

$$\mathbf{z}_k = h(\mathbf{x}_k, \mathbf{v}_k) \quad (5)$$

Here, the non-linear function h relates the a priori state \mathbf{x}_k and measurement noise $\mathbf{v}_k \sim N(0, R)$ to the expected measurements \mathbf{z}_k .

In the update step of the filter, external measurements of the robot state need to be integrated into the current estimate. For the purposes of the experiments presented here, the absolute position and orientation of the robot is measured through an external optical tracking system by Optitrack. Alternatively, a scan matching based approach with a mounted laser scanner could be used.

4.4 Augmented Extended Kalman Filter

The state vector $\mathbf{x} = [x, y, \theta]^T$ can be used to estimate the pose of the robot based on internal encoder and external tracking readings as outlined in Section 4.3.

If the values of the wheel diameters d_L and d_R and the wheel base b are known only approximately or are variable during robot operation, systematic errors will be injected into the estimation process. This will invariably lead to a degradation of Kalman Filter performance. Examples of systematic errors include unequal wheel diameters, wheel misalignment, and effective wheel base ambiguities due to non-point floor contact.

To alleviate that, the ideas from (Larsen, 1998) and (Martinelli et al., 2007) can be followed to augment the state vector by the unknown quantities. Deviating from this previous work, the wheel diameters and wheel base are added directly to the state vector instead of using an artificial multiplier. The augmented state vector is thus

$$\mathbf{x} = [x, y, \theta, d_L, d_R, b]^T \quad (6)$$

The linearized (6x6) system matrix can be derived based on the Jacobians of the non-linear function f in Equation (4). The partial derivatives can be readily found through symbolic differentiation in Matlab.

4.5 Experimental Validation

To validate the usefulness of the filter proposed in Section 4.4, the robot is driven multiple times along a circular path with a set of predetermined wheel velocities. Encoder readings of both wheels are recorded at 20 ms intervals.

The absolute position and orientation of the robot is determined by a mounted marker pattern that is tracked by an infrared camera system. The optical tracking data was logged and served as ground truth for this test run.

The test is performed at relatively slow speeds, so wheel slippage on the surface can be ignored. After the run concludes, the Augmented EKF is executed off-line on the log data. For the purposes of this evaluation, only the mean estimated values for wheel diameters d_L and d_R and wheel base b are used for further calculations.

As a baseline, d_L , d_R , and b were measured manually and the robot path was calculated through the dead reckoning equations (Equation (1) and Equation (2)). One would expect the shape of the resulting circle to closely resemble the shape recorded by the optical tracker.

To each set of circles, an ellipse was fitted and its measurements for major axis, minor axis and area were used as indicators for the validity of the estimated parameters. Table 1 shows the results of this run.

Table 1: The robot is driven along a circular path. Tracking data is collected and a dead-reckoned path is calculated for different values of wheel diameters and wheel base. The "Baseline" is measured manually ($d_L = d_R = 6.44$ cm, $b = 26$ cm), while the "Calibration" values are the mean output of the Augmented Extended Kalman Filter ($d_L = 4.647$ cm, $d_R = 4.517$ cm, $b = 26.98$ cm).

	Major Axis a (in cm)	Minor Axis b (in cm)	Ellipse Area (in cm ²)
Tracking Data (Ground Truth)	107.714	107.44	9089.235
Dead Reckoning (Baseline)	109.875	109.036	9409.337
Dead Reckoning (Calibration)	107.101	106.387	8948.930

Clearly, the quality of the dead reckoning improves with the newly calibrated values. This bodes well for the integration of the calibration into the virtual reality simulation of the mobile robot.

Although this experiment was performed off-line for convenience, the Kalman filter is designed to execute online while the robot is running and continuously update its estimates.

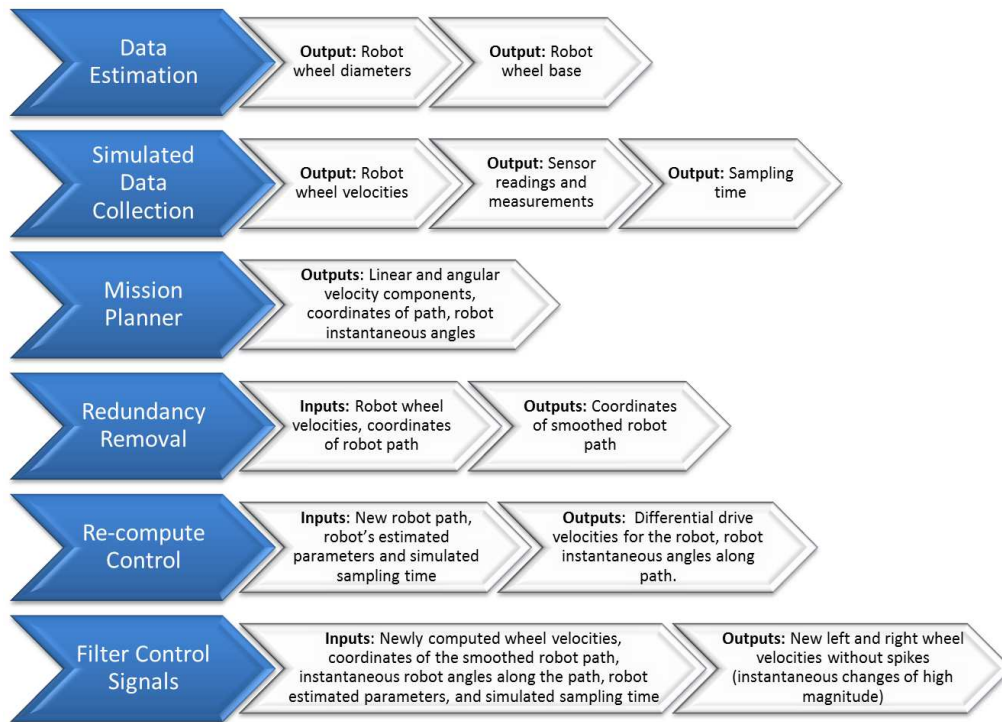


Figure 3: Planning and Execution Modules

5 PLANNING AND EXECUTION IN SIMULATION

The planning and execution stage is used on the master (simulation) side of the tele-operation to allow the operator to explore planning strategies and preview anticipated robot movements. This stage is divided into modules that are processed sequentially until a final successful behavior can be implemented on the real robot. Figure 3 depicts the six modules used during planning and execution, highlighting the inputs and outputs of each module. The absence of an explicit input indicates that this information directly flows in from the outputs of the module above it.

Data Estimation: The data estimation module is implemented according to the description in Section 4 i.e. the robot wheel diameters and wheel base are estimated using a Kalman Filter.

Simulated Data Collection: The data collection module logs all simulated data during a mission, including sampling time, left and right wheel velocities of the robot, encoder counts, and all readings of the mounted sensors.

Mission Planner: The mission planner integrates the estimated and simulated data to re-create the executed mission including generation of the coordinates of the robot path that must be passed as an input to the redundancy removal module.

Redundancy Removal: This module initializes regions of interest based on the definition of redundancy (user-specified). A matrix of distances between the coordinates on the redundant path is used to find pinch points (intersecting points) across the curves. These pinch points are used to delete any kinks or loops in the robot path, which are redundant.

Re-compute Control: The new path (time-series) is used to regenerate velocity vectors for the robot i.e. individual wheel velocities for the differential drive steering mechanism are re-computed based on the desired linear and angular velocities.

Filter Control Signals: The deletion of segments in the original path may result in the new path requiring instantaneous changes in robot velocity, leading to spikes in the control signal for each wheel. As a result of this deletion, the robot might be expected to be in a new position at the next sampling instant that is physically infeasible to attain. The path must therefore be re-interpolated between the regions where spikes occur, resulting in smoothed control signals for each robot wheel. For every control signal spike, the path of the robot is interpolated by increasing the travel-time between the spike-points. This involves a re-sampling of the position and velocity vectors of the robot to increase overall time for the mission. The orientation of the robot must be interpolated separately since simultaneous changes in position and ori-

entation of the robot can occur during the removal of kinks. Magnitude of velocity and angular velocity of robot are together used to determine left and right wheel velocities. The process is also iterative for each spike in the list, since the newly computed values for position and orientation are re-used in the interpolation process.

5.1 Case Study: Simple Wall Following Routine

A simulation scenario was created with a right-angled wall in the center of an indoor environment as shown in Figure 4. The simulated robot had a single infrared sensor mounted at its side at an acute angle, and a bump sensor. The robot utilized a differential drive steering and was programmed to perform a simple wall following routine. When the bump sensor was triggered on contact, it would cause the robot to reverse; following which it turned to its left and moved along the wall using a loosely tuned proportional controller acting on the error from the desired wall distance. The green dotted lines in the depiction indicate a rough path that the robot would follow when this algorithm was used. The red dots indicate regions where the robot would have to back up since the bump sensor was triggered.

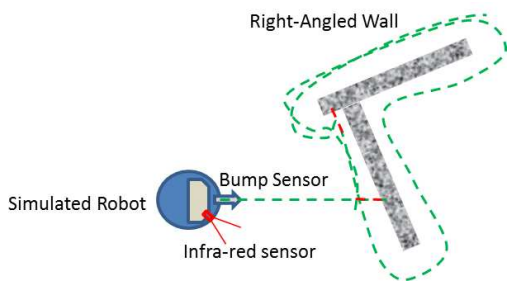


Figure 4: Simulation Setup

Figure 5(a) shows the left and right wheel velocities during the wall following routine. Figure 5 (b) shows the distance to the wall as measured by the on-board infrared sensor. A section of both graphs is magnified for closer examination (Figure 5(c) and Figure 5(d)). The data is generated by combining the **data estimation** and **simulated data collection** modules. The continuous oscillations to compensate for the wall distance-error highlights the implementation of the proportional controller. Notice that the high values of wall distance result in a corresponding difference in wheel velocities causing the robot to turn in an arc until the infrared sensor picks up the wall again.

Figure 6 (a) shows the actual path of the robot

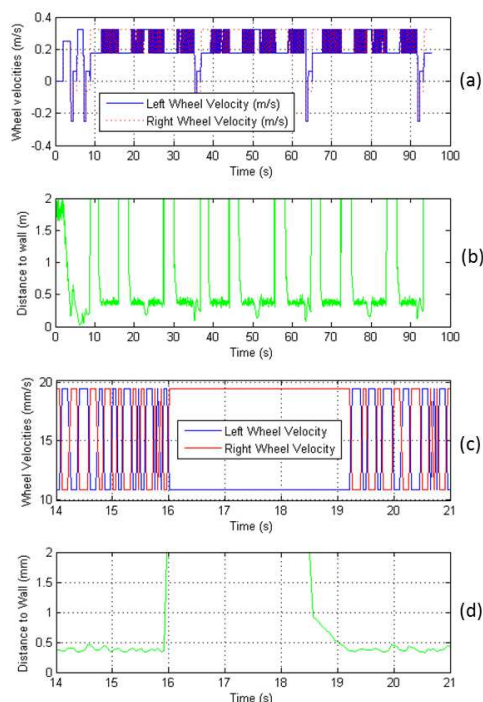


Figure 5: Wall Distance and Wheel Velocities. The graphs are described in detail in Section 5.1.

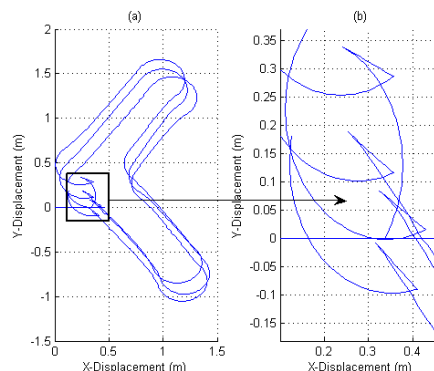


Figure 6: Path of Robot during wall-following

around the right-angled wall in the simulation. This is generated by the **mission planner** module. A portion of Figure 6 (a) has been zoomed into in Figure 6 (b) to show the redundant traversal of paths by the simulated robot. This occurs when the bump sensor makes contact with the wall and the robot backs up before turning away. In this case, redundancy is defined as a portion of the path that can be eliminated from the simulated path, without causing a change to the robot’s exploration route that would result in the oversight of valuable information. All sections of ‘bump and backup’ are therefore classified as redundant.

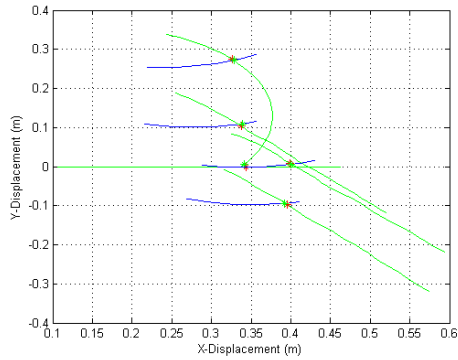


Figure 7: Regions of interest showing 'pinch points'.

Figure 7 shows the regions of interest identified based on the mission planner and the correspondingly computed pinch points. These pinch points are processed to delete redundant segments of the path in between. This task is performed by the **redundancy removal** module, resulting in a smooth path as shown in Figure 8 (a). The smooth path is passed as an input to the **re-compute control** module which calculates the wheel velocities required to achieve the new path. The module also notifies the **filter control signal** module of any instantaneous large changes required in the wheel velocities to help the robot achieve a specific position and orientation. These are shown in Figure 8(a). The filter control signal module then interpolates the path as described previously to help achieve a final smoothed path for upload to the main robot. The processed control signals (before and after removal of spikes) for each of the wheel modules is shown in Figure 9. It must be noted that in the newly calculated path (for upload to the real robot), there are no collisions with the wall, since this has already been compensated for from the information provided by the simulation.

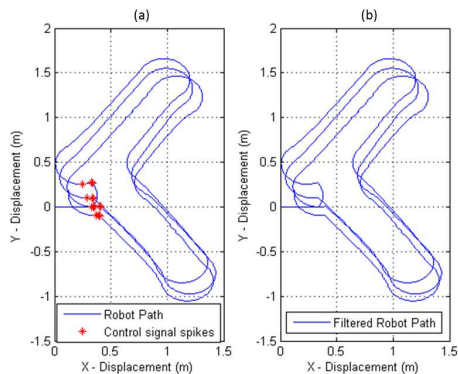


Figure 8: (a) Output from the re-compute control module indicating control signal spikes. (b) Filtered path after removal of control signal spikes by the final module

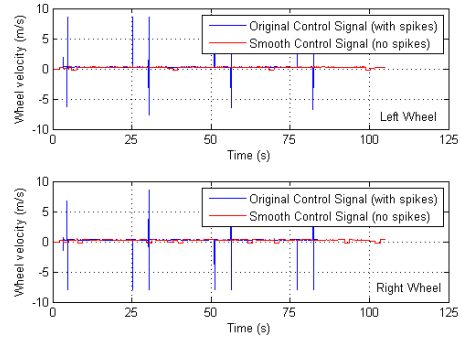


Figure 9: Control signal (wheel velocities) for the left and right wheels of the robot

6 EFFECT OF ERRORS IN PARAMETER ESTIMATION

The mission planning module relies on the estimated kinematic parameters to determine the robot's path in simulation. Specifically, the module integrates the wheel velocities over time to determine the path taken by the robot during the simulated mission. Errors in the kinematics therefore propagate through all the modules from an early stage. To illustrate this effect, the estimated wheel base value was modified by 4% on either side of the ideal value. The drift in the simulated path on either side of the actual path as shown in Figure 10 is a result of this error in the estimate. The mean squared errors between the actual path and the resultant error-ridden paths ($\pm 4\%$) are found to be 0.1043 m and 0.1033 m respectively, while the sums of absolute difference between the paths are found to be 198.6847 m and 196.7018 m correspondingly.

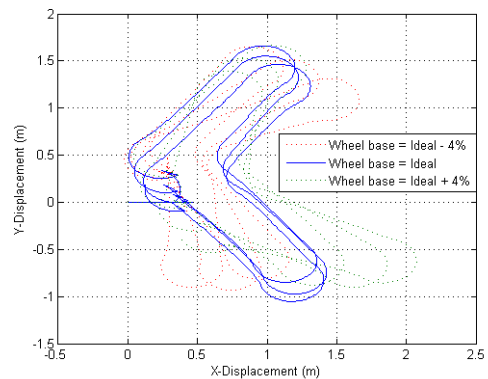


Figure 10: Effect of wrongly estimated wheel base

7 CONCLUSION AND FUTURE WORK

This paper presented a decoupled control paradigm for the tele-operation of mobile robots. The proposed control architecture benefits applications that have to deal with intermittent communication channels or varying time delays. A general system architecture has been described that integrates a virtual reality-based physical simulation and lends itself to rapid mission planning, modular development and distribution across a network. Preliminary experimental results on a sub-section of the control paradigm have been shown that demonstrate how kinematic parameters of a robot can be estimated and used to improve simulation results. In addition, an exemplar of a planning and execution module was described to emphasize the advantages of the presented system in comparison to traditional direct control paradigms.

Since the Augmented Extended Kalman Filter framework is in place, it can be integrated on the physical robot to continuously provide an updated robot state estimate. The presented framework can accommodate any numbers of sensor inputs, but fusing data from heterogeneous sources is a non-trivial problem and needs to be investigated. In particular, how the chosen robot path influences the evolution and error covariances of the estimates for the robot's kinematic parameters should be investigated.

In addition, the components of the system that have not been treated here, like environment modeling, slave-robot command execution and control need to be examined and integrated.

REFERENCES

- Anycode (2011). anyKode Marilou - Modeling and Simulation Environment for Robotics; Last accessed 2 January 2012. Available from: <http://www.anycode.com/index.php>.
- Arcara, P. and Melchiorri, C. (2002). Control schemes for teleoperation with time delay : A comparative study. *Robotics and Autonomous Systems*, 38:49–64.
- Bejczy, A., Kim, W., and Venema, S. (1990). The phantom robot: predictive displays for teleoperation with time delay. In *Proceedings, IEEE International Conference on Robotics and Automation*, pages 546–551. IEEE Comput. Soc. Press.
- Chong, N. Y., Kotokul, T., Ohba, K., Komoriya, K., Tanie, K., and Mechanics, E. (2000). Use of Coordinated On-line Graphics Simulator in Collaborative Multi-robot Teleoperation with Time Delay. In *Proc. IEEE International Workshop on Robot and Human Interactive Communication*, pages 167–172, Osaka, Japan.
- Hernando, M. and Gambao, E. (2007). Teleprogramming: Capturing the Intention of the Human Operator. In *Advances in Telerobotics*, volume 31 of *Springer Tracts in Advanced Robotics*, chapter 18, pages 303–320. Springer.
- Hokayem, P. and Spong, M. (2006). Bilateral teleoperation: An historical survey. *Automatica*, 42(12):2035–2057.
- Jackson, J. (2007). Microsoft robotics studio: A technical introduction. *Robotics & Automation Magazine, IEEE*, 14(4):82–87.
- Julier, S. and Uhlmann, J. (2004). Unscented filtering and nonlinear estimation. *Proceedings of the IEEE*, 92(3):401–422.
- Kalman, R. E. (1960). A New Approach to Linear Filtering and Prediction Problems. *Journal of Basic Engineering*, 82(Series D):35–45.
- Kheddar, A. (2001). Teleoperation based on the hidden robot concept. *Systems, Man and Cybernetics, Part A: Systems and Humans, IEEE Transactions on*, 31(1):1–13.
- Kheddar, A., Neo, E., Tadakuma, R., and Yokoi, K. (2007). Enhanced Teleoperation Through Virtual Reality Techniques. In Ferre, M., Buss, M., Aracil, R., Melchiorri, C., and Balaguer, C., editors, *Advances in Telerobotics*, volume 31 of *Springer Tracts in Advanced Robotics*, chapter 9, pages 139–159. Springer.
- Larsen, T. (1998). *Optimal Fusion of Sensors*. Phd thesis, Technical University of Denmark.
- Martinelli, A., Tomatis, N., and Siegwart, R. (2007). Simultaneous localization and odometry self calibration for mobile robot. *Autonomous Robots*, 22(1):75–85.
- Michel, O. (2004). Webots TM : Professional Mobile Robot Simulation. *International Journal of Advanced Robotic Systems*, 1(1):39–42.
- Pan, Y.-j., Canudas-de wit, C., and Sename, O. (2006). A New Predictive Approach for Bilateral Teleoperation With Applications to Drive-by-Wire Systems. *Robotics, IEEE Transactions on*, 22(6):1146–1162.
- Wang, C. (1988). Location estimation and uncertainty analysis for mobile robots. In *Proceedings. 1988 IEEE International Conference on Robotics and Automation*, pages 1231–1235. IEEE Comput. Soc. Press.
- Wright, B. Y. J., Hartman, F., Cooper, B., Maxwell, S., Yen, J., and Morrison, J. (2006). Driving on Mars with RSVP - Building Safe and Effective Command Sequences. *Robotics & Automation Magazine, IEEE*, 13(2):37 – 45.
- Yu, C.-q., Ju, H.-h., Gao, Y., and Cui, P.-y. (2009). A Bilateral Teleoperation System for Planetary Rovers. In *2009 International Conference on Computational Intelligence and Software Engineering*, pages 1–5. IEEE.
- Zhu, J., He, X., and Gueaieb, W. (2011). Trends in the Control Schemes for Bilateral Teleoperation with Time Delay. *Autonomous and Intelligent Systems*, 6752:146–155.